

About Exobiology: The Case for Dwarf K Stars

M. Cuntz¹ and E. F. Guinan²

¹*Department of Physics, University of Texas at Arlington,
Arlington, TX 76019, USA*

cuntz@uta.edu

²*Department of Astrophysics and Planetary Science, Villanova University,
Villanova, PA 19085, USA*

edward.guinan@villanova.edu

ABSTRACT

One of the most fundamental topics of exobiology concerns the identification of stars with environments consistent with life. Although it is believed that most types of main-sequence stars might be able to support life, particularly extremophiles, special requirements appear to be necessary for the development and sustainability of advanced life forms. From our study, orange main-sequence stars, ranging from spectral type late-G to mid-K (with a maximum at early-K), are most promising. Our analysis considers a variety of aspects, including (1) the frequency of the various types of stars, (2) the speed of stellar evolution their lifetimes, (3) the size of the stellar climatological habitable zones (CLI-HZs), (4) the strengths and persistence of their magnetic dynamo generated X-ray–UV emissions, and (5) the frequency and severity of flares, including superflares; both (4) and (5) greatly reduce the suitability of red dwarfs to host life-bearing planets. The various phenomena show pronounced dependencies on the stellar key parameters such as effective temperature and mass, permitting the assessment of the astrobiological significance of various types of stars. Thus, we developed a “Habitable-Planetary-Real-Estate Parameter” (HabPREP) that provides a measure for stars that are most suitable for planets with life. Early K stars are found to have the highest HabPREP values, indicating they may be “Goldilocks” stars for life-hosting planets. Red dwarfs are numerous, having long lifetimes, but their narrow CLI-HZs and hazards from magnetic activity make them less suitable for hosting exolife. Moreover, we provide X-ray–FUV irradiances for G0 V – M5 V stars over a wide range of ages.

Subject headings: astrobiology – stars: activity – stars: late-type – stars: luminosity function, mass function, X-ray–UV Irradiances – planetary systems

1. Introduction

Since the discovery of the first planet hosted by a Sun-like star was found more than 20 years ago orbiting 51 Pegasi (Mayor & Queloz 1995), the search for life in the Universe has received unprecedented attention. It is now unequivocally the most fundamental task of astrobiology, with significant ramifications toward other fields such as astronomy, astrophysics, microbiology, planetary and atmospheric science, and geodynamics. Generally, the search for life around stars, notably F–M type main-sequence stars, is mostly concentrated on two pivotal aspects. The first aspect deals with the identification of stars suitable to offer sustained habitable environments, whereas the second aspect focuses on planets through elucidating which planetary properties make them (potentially) habitable. Previously, significant progress has been made on both aspects, including work by Scalo et al. (2007), Lammer et al. (2009, 2013), Horner & Jones (2010), Rugheimer et al. (2013), Kasting et al. (2014), among others.

Regarding the stellar aspect, a central theme is the identification of the existence and stability of climatological habitable zones (CLI-HZs) aimed at rocky planets of different sizes; see, e.g., Kaltenegger et al. (2012) for a updated classification scheme. Previous results pertaining to single stars have been obtained by, e.g., Kasting et al. (1993), Kopparapu et al. (2013, 2014) and for higher-order (binary and multiple) systems by, e.g., Cuntz (2014, 2015). Furthermore, the impact of stellar evolution on the CLI-HZs has been explored as well (e.g., Underwood et al. 2003; Rushby et al. 2013). These studies show that when stars evolve and increase in luminosity with age, the CLI-HZs broaden and move outward. Recent work by Kasting et al. (2014) considers updated CLI-HZ boundaries based on improved planetary climate models and discusses remote life-detection criteria. For example, for the case of the Earth, the expected increase in the luminosity of the Sun over the next $\sim 1\text{--}2$ Gyr will result in the Earth no longer comfortably residing within the solar CLI-HZ.

Other efforts concentrate on suitable stellar properties that are able to provide favorable biospheric conditions for hosted planets. This kind of work explores the magnitude and temporal evolution of stellar magnetic-dynamo driven activity, such as UV, EUV, and X-ray radiative emission (e.g., Güdel et al. 1997; Guinan & Ribas 2002; Ribas et al. 2005; Tu et al. 2015) and (super-)flares (e.g., Hawley et al. 2003; Maehara et al. 2012; Guinan et al. 2016). Guinan et al. (2003) pointed out that for solar-like stars, the FUV and X-ray emissions of the young (age ~ 100 Myr) Sun could have been higher by 30–50 times and 100–500 times, respectively, than today. Generally, stellar activity is a crucial feature of all late-type stars and most pronounced in M dwarfs; it subsides as stars age. For solar-type and cooler stars (i.e., stars with outer convective zones), this process is attributable to stellar angular evolution owing to internal changes and to magnetized winds (e.g., Keppens et al. 1995;

Charbonneau et al. 1997).

The aim of this work is to consider detailed knowledge about stars including their relationships to planets to evaluate which types of stars constitute the best and most likely candidates for the facilitation of long-term exobiology. In Sect. 2, we discuss the amounts of habitable planetary real estate, as determined by the sizes of the CLI-HZs and the relative frequency of the various types of stars. In Sect. 3, we consider stellar activity, i.e., high energetic stellar radiation, flares, superflares, and winds regarding their relevance to the circumstellar environments. The overall assessment of habitability, i.e., “the big picture”, is conveyed in Sect. 4.

2. Habitable Planetary Real Estate Parameter (HabPREP)

In the following, for the different types of main-sequence stars, we focus on the size of the CLI-HZs and their relative frequency to evaluate amounts of habitable planetary real estate. Other aspects such as the impact of magnetic-dynamo driven stellar activity will be considered in Sect. 3. Previously, Kasting et al. (1993) utilized 1-D climate models, which were state-of-the-art at the time, to compute the CLI-HZs for a domain of main-sequence stars with spectral-types ranging from late F to early M. The basic premise of their work was the assumption of an Earth-type planet with a CO₂/H₂O/N₂ atmosphere and, moreover, that habitability requires the presence of liquid water on the planetary surface. This work was significantly improved through subsequent studies, including the recent work by Kopparapu et al. (2013, 2014). Their approach encompassed numerous improvements, including the consideration of revised H₂O and CO₂ absorption coefficients.

For example, the work by Kopparapu et al. (2013, 2014) re-computes the recent Venus / early Mars (RVEM) limits of the CLI-HZ introduced by Kasting et al. (1993). For a solar-like star, the range of the RVEM extends from 0.75 to 1.77 au. Other limits regarding the CLI-HZs are based on the runaway greenhouse effect (inner limit) and maximum greenhouse effect (outer limit); in the following, these limits are used to signify the general habitable zone (GHZ). At the inner limit, the greenhouse phenomenon is enhanced by water vapor, thus promoting surface warming, which increases the atmospheric water vapor content, thus further raising the planet’s surface temperature. Eventually, this will lead to the rapid evaporation of all surface water. For the outer limit, it is assumed that a cloud-free CO₂ atmosphere shall still be able to provide a surface temperature of ~ 273 K (0° C).

For solar-like stars, and assuming an Earth-mass object, Kopparapu et al. (2013, 2014) identified the GHZ limits as approximately 0.95 and 1.68 au. In contrast, Kasting et al.

(1993) identified them as 0.84 and 1.67 au, respectively. Another limit of habitability is given as the moist greenhouse limit, which for stars akin to the Sun has been updated to 0.99 au. In the previous work by Kasting et al. (1993) another limit was identified given by the first CO₂ condensation obtained by the onset of formation of CO₂ clouds at a temperature of 273 K, which has not been supported by Kopparapu et al. (2013, 2014). Nevertheless, in the present work, the moist greenhouse limit and the limit due to the first CO₂ condensation are used to define the conservative habitable zone (CHZ), as motivated by a large array of previous studies. Note that in the work by Kopparapu et al. (2013, 2014) the CLI-HZ given by the RVEM limits is referred to as GHZ, whereas the CLI-HZ between 0.95 and 1.68 au, as identified for an Earth-mass planet, is referred to as CHZ. This notation is different from that of the present study, which however closely follows previous conventions (see Table 1).

Results are given in Table 2. An important aspect is that compared to previously published versions of that figure, updates have been made for stars of $T_{\text{eff}} \lesssim 4500$ due to improved spectro-thermometry in consideration of updated PHOENIX atmosphere models (Husser et al. 2013; Mann et al. 2013), resulting in revised values for effective temperature, radius, mass, and luminosity. These results have been utilized for the assessment and interpretation of *Kepler* field planet-hosting candidates. We also evaluated the stability of the CLI-HZs for stars with spectral types from \sim F5 V to \sim M5 V (see Table 2). In this case, we explored when the inner limit of the CHZ / GHZ overtakes the outer limit with the latter recorded at the beginning of stellar main-sequence evolution. This time of t_{ev} , usually referred to as timescale of the continuous habitable zone (in reference to CHZ or GHZ), describing the region (or duration of time) when a planet can be continuously habitable (i.e., able to maintain liquid water on its surface) is relatively short for early and mid F-type stars, see also Sato et al. (2014) for further results, but very prolonged for the more slowly evolving, cooler, low-mass main-sequence K- and M-type stars. For example, for K2 V stars, t_{ev} is identified as \sim 22 and \sim 32 Gyr for the CHZ and GHZ, respectively, which is more than a factor of 3 longer than for G2 V stars like the Sun. For low-mass M-type stars (i.e., red dwarfs; $T_{\text{eff}} \lesssim 3800$ K), t_{ev} is found to exceed 100 Gyr.

Next, we focus on the relative frequency of stars, as obtained by the initial mass function (IMF); see Figure 1 and 2. In this regard, it is found that low-mass stars are much more frequent than high-mass stars given by the shape of the IMF (e.g., Kroupa 2001, 2002; Chabrier 2003; Chabrier et al. 2005). The number of stars strongly increases with decreasing stellar mass (albeit uncertainties associated with the region of formation, stellar metallicity, etc.), although the IMF shows some flattening for stellar masses below $\sim 0.5 M_{\odot}$ (i.e., mid and late M-dwarfs), if displayed against $\log M$ with M as stellar mass. The IMF typically follows a broken power law, which is an empirical function describing the distribution of initial masses for a stellar population. More than 75% of stars are identified as M-dwarfs. Early work

establishing the IMF has been given by, e.g., Muench et al. (2000), Lucas & Roche (2000), Hillenbrand & Carpenter (2000), and Luhman et al. (2000), which focused on distinct stellar clusters including clusters located in the Orion and Taurus constellation; some of this work also employed the *Two-Micron All Sky Survey* (2MASS). Several decades ago, Miller & Scalo (1979) pointed out that the flattening of the IMF in the regime of very low mass stars may be due to the mutual interactions between the fragments of interstellar clouds as well as their interactions with the ambient gas rather than cloud fragmentation itself. Later on, this interpretation has been backed up by detailed numerical simulations given by, e.g., Clark et al. (2008), which also allowed to link the variations of the initial IMF to the rate of star formation. Note that the general behavior of the IMF as obtained is also consistent with the number count of stars in the solar neighborhood, i.e., the RECONS project¹ (Henry 2009; Henry & Jao 2015).

Forming the product between the sizes of the CLI-HZs and the relative frequency of stars allows to describe the “Habitable-Planetary-Real-Estate Parameter” (HabPREP) for the different types of main-sequence stars². The results reveal a maximum for stars with effective temperatures between about 4900 K and 5300 K (i.e., K2 V – G8 V stars) and a strong increase for M dwarfs of effective temperatures less than about 4000 K. The overall behavior of HabPREP is determined by two separate trends. First, the width of the CLI-HZs steadily decreases as a function of decreasing effective temperature or mass. Second, the relative frequency of stars according to, e.g., Kroupa (2002) and Chabrier (2003), and first increases, but then near $0.5 M_{\odot}$ (with the exact value dependent on the set of observational data and the particulars of the statistical approach) levels off or starts to decrease (if displayed against $\log M$ with M as stellar mass); both behaviors combined result in a maximum for HabPREP as said (see Figure 1). HabPREP is normalized to unity for G2 V stars, following the IMF obtained by Chabrier et al. (2005), based on the GHZ as choice for the CLI-HZ. However, the general behavior of the HabPREP function (e.g., position of its maximum) shows little dependence on the type of CLI-HZ selected; see Figure 2 for details. As discussed in Sect. 3, M dwarfs (even though preferred by HabPREP) will be ruled less favorable for providing habitable environments compared to orange dwarfs of spectral type late-G to mid-K owing to their excessively high amounts of activity.

¹For more information, and regular updates, visit <http://www.recons.org>.

²Strictly speaking, the definition of HabPREP should also consider the timescale of stability for the continuous habitable zone, t_{ev} . However, the omission of this step will not affect our conclusions in a notable manner. Stars between spectral type late-G and M have highly stable CLI-HZ (see Table 2), whereas F-type stars as well as early and mid-G stars have not. Thus considering the impact of t_{ev} regarding HabPREP would make the maximum between stellar types G8 V and K2 V even more pronounced.

3. Impact of High Energy X-ray–UV Radiation, (Super-)Flares and Winds

Next we discuss the impact of high energy radiation, flares, and winds on the prospect of habitability for HZ planets hosted by G- to M-type stars. There is a number of earlier studies of solar-type stars on the influence of dynamo-generated energetic radiation encompassing various wavelength regimes, especially X-ray, extreme-UV (EUV) and far-UV (FUV) as well as stars of different ages (e.g., Güdel et al. 1997; Guinan & Ribas 2002; Guinan et al. 2003; Ribas et al. 2005). Previously, Ribas et al. (2005) presented results from the “Sun in Time” program indicating that the coronal–transition region X-ray–EUV ($\sim 1\text{--}910 \text{ \AA}$) emissions of the young main-sequence Sun were ~ 100 (EUV) to ~ 600 (X-ray) times stronger than those of the present Sun. Similarly, the transition region and chromospheric FUV–UV emissions of the young Sun³ were identified to be 20–60 and 10–20 times stronger, respectively, than at present.

Even though Earth is a striking counterexample as it was able to survive significant energetic radiation and wind flows from the early Sun owing to magnetic protection (e.g., Grießmeier et al. 2004), high levels of stellar activity are typically considered a significant hindrance to the development and sustainability of advanced exobiology. Thus, we should also consider the adverse effects that the active young Sun had on the two other initial solar-HZ planets. Because of high levels of magnetic activity of the early Sun, Venus lost its original water inventory very early and now is a very hot, dry, inhospitable planet (e.g., Kulikov et al. 2006). Also, because of the Sun’s past high activity, coupled with the loss of its protective geomagnetic field some 3.5 Gyr ago, Mars today is too cold and dry for complex life at least on its surface (e.g., Fairén et al. 2010). Thus, it could be considered very fortunate that the Earth’s atmosphere, water inventories and life survived, persisted, and evolved in spite of the harsh effects of the active early Sun as well as the devastating effects of impacts of asteroids and comets. Therefore, in the view of Fermi’s paradox, i.e., no signs or signals of advanced life, see Chopra & Lineweaver (2016) for recent discussions, complex life could indeed be very rare.

In this study we mostly focus on stellar coronal X-ray and chromospheric Ly- α fluxes of G0 V - M5 V stars over a wide age range (see Figure 3). Ly- α serves as an excellent indicator for FUV emission because this emission line alone contributes 80–90% of the total stellar

³Based on studies by, e.g., Schröder & Smith (2008) and Mowlavi et al. (2012) it has been found that the effective temperature of the young Sun was $\sim 5600 \text{ K}$ (G6–7 V). This value is fairly close to the upper limit of the range of stars regarded as favorable for supporting complex life forms (see Sect. 4), although the emergence of sophisticated life on Earth occurred at a considerably later stage when the solar temperature and luminosity had increased.

FUV (1150–1750 Å) flux (e.g., Linsky et al. 2013). Emphasis is placed on young stars (< 1 Gyr), when fast rotation generates strong magnetic fields, which give rise to high levels of X-ray and FUV emission. A study of the X-ray and Ly- α properties of M-stars over a wide range of ages has recently been carried out by Guinan et al. (2016). In this study the X-ray and FUV Ly- α fluxes, i.e., f_X and $f_{Ly\alpha}$, were determined for a sample of M0-5 V stars with ages from 0.1–11.5 Gyr for a nominal reference distance of 1.0 au (and also for 0.17 au, the mid CLI-HZ for a \sim M1 V star). For young M-stars (ages < 500 Myr) the X-ray and $f_{Ly\alpha}$ CLI-HZ irradiances are both very high and comparable in strength. As noted in this study, the FUV Ly-alpha flux dominates the FUV flux, comprising 80–90% of the total 900–1800 Å FUV flux and can thus be used to estimate the total FUV irradiance. In the following, we extend the study of X-ray and FUV (given by Ly- α) irradiances of M-stars as a function of age, to more massive and luminous G and K stars.

Note that the H I Ly- α 1215.67 Å emission line is by far the strongest emission feature in the solar EUV–FUV (~ 100 –1700 Å) spectrum of the Sun (Tian 2013), and it is dominant in the EUV–FUV regime of other solar-type (G stars) and cooler K and M main-sequence stars as well. Also, Ly- α emission is the main contributor to the heating, ionization and photochemistry of the upper atmosphere of the Earth as well as of many solar-system planets and moons (Holland 1984); recent results have also been obtained for planets in exosolar systems (e.g., Miguel et al. 2015). For Earth, the Ly- α flux plays a major role in the photodissociation of important molecules such as H₂O, CO₂, CH₄, O₂, and O₃ in planetary atmospheres. Fortunately, reliable measures of Ly- α emission fluxes have meanwhile become available, obtained with HST (see, e.g., France et al. 2013; Linsky et al. 2013). These stellar Ly- α integrated fluxes have been reconstructed from HST-STIS and COS spectra for a sample (~ 50) of main-sequence F5 – M5 stars (Linsky et al. 2013; Guinan et al. 2016).

Similar to the M-star study of Guinan et al. (2016), we utilize the Ly- α and X-ray flux measures of G and K stars obtained by Linsky et al. (2013). (Note that these authors report those fluxes for a reference distance of 1.0 au from the star but they can easily be transformed to any other distance following the inverse square law.) These X-ray fluxes were supplemented by additional X-ray measures found in the literature, previously obtained with ROSAT, XMM-Newton or Chandra. Ages were estimated from open cluster (such as Pleiades and Hyades) or moving group memberships (such as the Ursae Majoris Moving Group), stellar rotation rates (through employing rotation–age relations) or from memberships in wide binary systems (such as Proxima Centauri) in which one component has an isochronal or asteroeismic age measures (e.g., α Cen). X-ray fluxes are available for a large number of stars from all-sky X-ray surveys like ROSAT as well as from more recent X-ray observations by Chandra and XMM-Newton. Mean milestone age baseline X-ray flux–age calibrations of G and K stars were obtained from ROSAT studies of Pleiades cluster (age ~ 0.1 Gyr)

and Hyades cluster (age ~ 0.65 Gyr) carried out by Micela et al. (1990) and Stern et al. (1995), respectively. These were supplemented by relations given by Basri et al. (1996), Perryman et al. (1998), and Mamajek & Hillenbrand (2008).

Based on our exobiological perspective, we focus on planets at an Earth-equivalent distance⁴, also referred to as homeothermic distance (HTD), which for M0-6 dwarfs ranges between ~ 0.20 and ~ 0.05 au; information for various stars is given in Figure 4 and Table 3. Our analysis also takes into account different L_X – age relations, which for G and M dwarfs have been obtained by Güdel (2007) and Guinan et al. (2016), respectively. In addition, X-ray and FUV ($\text{Ly-}\alpha$) flux calibrations were made for K-stars in similar manner as was done for M-stars. For intermediate stellar types adequate interpolation is used. Data for stellar activity at ages of ~ 5 Gyr are based on the Sun, 18 Sco, α Cen A & B, Proxima Cen, and 40 Eri A & C. As shown in Figure 3 and 4, our analysis shows that for low-mass stars (especially stars cooler than $\sim M3$ V), the amounts of planetary X-ray and FUV irradiance at HTDs are drastically increased due higher X-ray–FUV emissions of young stars and the closeness of the HTDs (i.e., < 0.2 au) to their host stars. Although in Table 3 we give the X-ray and FUV ($\text{Ly-}\alpha$) fluxes at the stellar HTDs, they can also be applied to any other distance following the inverse square law. Since the $\text{Ly-}\alpha$ emission flux contributes 80–90% of the total FUV flux, multiplying the $\text{Ly-}\alpha$ flux by ~ 1.15 should yield a good approximation for the total.

As given in Table 3, and shown in Figure 3, the X-ray and $\text{Ly-}\alpha$ HTD fluxes are comparable for young stars (age < 0.65 Gyr) of all spectral types. At an age of 0.1 Gyr, the X-ray HTD fluxes are ~ 1.5 – $2.0\times$ higher than the corresponding HTD $\text{Ly-}\alpha$ fluxes. However, by an age of about 5 Gyr, the $\text{Ly-}\alpha$ HTD fluxes are approximately 10–30 times larger than the corresponding X-ray HTD fluxes across all spectral types. Thus, we find that for older G–M stars, the $\text{Ly-}\alpha$ HTD fluxes dominate the X-ray–FUV spectral region. It is also seen that the largest changes with stellar age occur for the X-ray HTD fluxes. For example, for solar-type G2–8 V stars, the HTD X-ray flux is $\sim 400\times$ higher for very young (0.1 Gyr) stars relative to older stars at ages of 5 Gyr.

The HTD X-ray and $\text{Ly-}\alpha$ fluxes are very high for stars cooler than about M3 V compared to G and K stars of corresponding ages (see Figure 3). For example, compared to a

⁴Earth-equivalent distances mostly depend on the stellar luminosity but the stellar effective temperature needs to be considered as well. For example, K and M-dwarfs have more emission in the near-IR compared to G-dwarfs, and a planet can absorb more near-IR radiation from water-vapor around K and M-dwarfs making them warmer at an Earth-equivalent distance if no effective temperature correction for that distance is applied. Previously, corrective formulae were given by Underwood et al. (2003) and Selsis et al. (2007) that are used by us, including recasting in response to the studies of Kopparapu et al. (2013, 2014).

young (0.1 Gyr) G2 V star, the HTD X-ray flux for an M4–5 V star ($T_{\text{eff}} \sim 3200$ K) is over $45\times$ higher. This is primarily due to the very small values of HTDs for these low-luminosity stars with $\text{HTD} < 0.15$ au as well as their more efficient magnetic dynamos due to their deep convective zones. To illustrate this, a HTD planet hosted by a solar-age (~ 5 Gyr) M5–6 V star (e.g., Proxima Cen and Wolf 359) would receive over $\sim 400\times$ and $\sim 60\times$ more X-ray and FUV radiation, respectively, than the Earth presently receives from the Sun. As shown in Table 2, at younger ages (~ 0.1 Gyr) the HTD X-ray and FUV irradiances experienced by planets hosted by M4–5 V red dwarfs are expected to be even higher. For example, the X-ray and FUV HTD fluxes for these red dwarfs are inferred as $\sim 55\times$ and $\sim 6\times$ higher, respectively, at 0.1 Gyr compared to ages of ~ 5 Gyr; furthermore, if compared to the irradiance of today’s Earth, they are elevated by even much higher factors, which are ~ 350 and $\sim 20,000$ or more, respectively.

Another aspect of stellar activity pertains to flares and superflares. Superflares are defined as having total energies of $E > 10^{33}$ ergs (see Maehara et al. 2012). Generally, it has been found that flares are most intense and frequent in young stars and stars of late spectral types, notably M-dwarfs. Aside from the flare properties (i.e., strength, spectral energy distribution, frequency, stochasticity) effects on Earth-type planets in CLI-HZs are heavily determined by the CLI-HZ’s proximity, i.e., the very small values for the HTDs for those stars. Thus, detailed studies about the impact of flares on possible exolife entail outcomes that are unfavorable or mixed at best (e.g., Segura et al. 2010; Kastning et al. 2014). Superflares as given by *Kepler* data are found for stars of spectral types of G to M. For example, Candelaresi et al. (2014) reported that from the more than 100,000 stars included the study, 380 show superflares with a total of 1690 such events. With decreasing effective temperature, an increase in the superflare rate is observed, which is consistent to previous findings, and in alignment to dynamo theory. They also conclude that the resulting statistics of the dissipation energy is similar to the observed flare statistics as a function of the inverse Rossby number. From the perspective of this study, superflares are expected to be most significant for Earth-equivalent planets in the consideration of their close proximity to the stars, i.e., small HTDs. The effects of flares on habitability of planets is complex and beyond the scope of this paper; it will be considered by us in a subsequent paper.

Dense stellar winds (as present in active young stars) are also expected of having an adverse impact on circumstellar habitability (Johnstone et al. 2015). Lammer et al. (2003) showed that the combination of high X-ray–UV irradiance and strong (more dense) stellar winds expected from young G, K, and M dwarfs can, via ion-pickup mechanisms, act synergically to strip away atmospheres of close-in planets (e.g., Vidal-Madjar et al. 2003). Unless a hosted CLI-HZ planet has a strong and persistent magnetic field, amounting to a protective magnetosphere, there is a significant possibility that the planet will lose most, if not all,

of its atmosphere including its water inventories (e.g., Grießmeier et al. 2004). In our solar system, the early loss of water on Venus (Kulikov et al. 2006) and ~ 1 Gyr later on Mars (e.g., Fairén et al. 2010, and references therein) are best explained by the lack of strong, sustained geomagnetic fields on these planets. However, currently we are not in the position to include stellar mass loss fluxes in this study largely because it is still uncertain how the stellar wind properties change with spectral type and age. For example, the most recent wind measurement for κ Ceti (G5 V), a young (~ 0.7 Gyr) solar-type star, by do Nascimento et al. (2016) indicates a mass loss rate of ~ 50 times the present Sun. This result agrees very well with recent wind density estimates of solar-type stars with age by Airapetian & Usmanov (2016). Since stellar winds scale to magnetic fields and activity (e.g., Schrijver et al. 2003; Preusse et al. 2005; Cranmer & Saar 2011), it can be assumed that winds are most dense in young, magnetically active stars and planets at close-in HTDs (as given for late-K and M dwarfs) are most affected.

4. The Big Picture

The aim of this work is a multi-facet attempt to identify types of stars consistent with the durable existence of life, notwithstanding extremophiles, for which according to terrestrial analyses (e.g., Rothschild & Mancinelli 2001) large windows of opportunities might exist. General stellar aspects motivate us to focus on the main-sequence rather than pre- or post-main-sequence scenarios, which are typically of highly transitory nature. Aspects of primary importance include the frequency of the various types of stars, the size of the stellar CLI-HZs, and the rapidness of stellar evolution for various types of main-sequence stars. Following previous work by, e.g., Kopparapu et al. (2013, 2014) that indicates the decrease in the size of the CLI-HZs with decreasing stellar mass, luminosity and effective temperature – irrespectively of the planetary climatological criteria for defining the CLI-HZ limits – tend to favor higher-mass stars. That is F–G-type stars have wide CLI-HZ limits whereas lower mass mid-K and M-type stars have narrow CLI-HZs located close to the star. Low-mass stars, however, are much more frequent than high-mass stars as given by the shape of the IMF (e.g., Kroupa 2001, 2002; Chabrier et al. 2005). The total number of stars greatly increases with decreasing stellar mass, although there is an onset of flattening or modest decrease for masses below $\sim 0.5 M_{\odot}$. Hence, more than 75% of stars are identified as M-type dwarfs. This result is also consistent with the number count of stars in the solar neighborhood, i.e., the RECONS project (Henry 2009; Henry & Jao 2015).

Based on the combined behaviors of the CLI-HZs and the IMF, we are able to conclude that, from a statistical perspective, orange dwarf stars, ranging from spectral type

late-G to mid-K are most promising regarding long-term exobiology. More massive stars ($M \gtrsim 1.3 M_{\odot}$), such as F-type stars, are known to rapidly evolve away from the main-sequence (e.g., Meynet et al. 1993; Mowlavi et al. 2012), a significant disadvantage for the evolution and sustainment of exolife, though limited opportunities for circumstellar habitability may still exist (e.g., Cockell 1999; Sato et al. 2014). Regarding M-type dwarfs, numerous studies have been pursued about the prospects of providing habitable environments (e.g., Segura et al. 2005; Lammer 2007; Tarter et al. 2007; Scalo et al. 2007; Lissauer 2007; Kasting et al. 2014). Generally, these studies convey multiple adverse aspects regarding supporting habitable environments, including (but not limited to) intense high-energy radiative emissions, strong stellar flares, the narrowness of the CLI-HZ, and possible geodynamic planetary insufficiencies (e.g., lack of volatiles).

To date, there has been a large array of research targeting both flares and energetic radiation for stars of different ages and spectral types. Examples of flare studies include work by, e.g., Hawley et al. (2003), Robinson et al. (2005), and Davenport et al. (2012). Generally, it has been found that flares are most intense and frequent in young stars and stars of late spectral types, notably M-dwarfs (e.g., Feigelson et al. 2007). Aside from the flare properties (i.e., strength, spectral energy distribution, frequency, stochasticity) effects on Earth-type planets in CLI-HZs are heavily determined by the CLI-HZ’s proximity, i.e., the small values (< 0.2 au) for the HTDs of those stars. Thus, detailed studies about the impact of flares on possible exolife entail outcomes that are unfavorable or mixed at best (e.g., Segura et al. 2010; Kasting et al. 2014). Superflares revealed by *Kepler* data are found for stars of spectral types of G to M, but again are expected to have most adverse impacts for planets of M-dwarfs. A large number of superflares have also been detected for solar-type stars (e.g., Maehara et al. 2012, 2015; Shibayama et al. 2013; Katsova & Livshits 2015). Surprisingly, superflares may have favorable ramifications for possible exolife around G-type (and perhaps early K-type) stars (Airapetian et al. 2016), as they might trigger the production of hydrogen cyanide (HCN), an essential molecule of prebiotic chemistry.

In the present work, we focus on the X-ray and FUV Ly- α irradiances for planets in the CLI-HZ, notably located at the HTD for stars of different effective temperatures, luminosities, and ages. For most stars the X-ray fluxes dominate the EUV fluxes and the Ly- α emission fluxes dominate in the FUV region and thus are both critical (see Table 3 and Figure 3). Ultimately, high levels of energetic radiation lead to significant planetary atmospheric evaporation, as discussed by, e.g., Lammer et al. (2003), Vidal-Madjar et al. (2003), and Penz & Micela (2008). This behavior entails adverse consequences for the habitable environments of late-K and M dwarfs (see Figure 4), which is in part also caused the very close proximity of the CLI-HZs. Additionally, as argued by Raymond et al. (2007), there is a decreased probability of habitable planet formation around those stars. It has

also been pointed out that accreting planets, if formed, subsequently located in the CLI-HZ around stars cooler than K5 (including the full range of M-dwarfs) are most likely subjected to runaway greenhouse processes, and thus may lose substantial amounts of water initially delivered to them (Ramirez & Kaltenegger 2014; Luger & Barnes 2015; Tian & Ida 2015), thus emerging as (almost certainly) uninhabitable dry planets (“desert worlds”). Particularly, Tian & Ida (2015) argued that Earth-mass planets with Earth-like water contents orbiting M-dwarfs have a 10–100 times reduced likelihood than around G dwarfs.

The results for red dwarfs, as discussed, add further exobiological relevance in support of late-G to mid-K orange dwarfs (i.e., T_{eff} between approximately 4900 K and 5300 K) as more likely hosts for planets supporting complex life. Another intriguing aspect that also tends to support our main conclusion is the onset of tidal locking, which for planets located in the CLI-HZ (both CHZ and GHZ), pertaining to a timescale of ~ 4.5 Gyr, occurs for stars with effective temperatures close to 4800 (± 200) K (i.e., for $\sim K3$ V stars). This indicates that for planets hosted by stars hotter and more luminous, due to their more distant CLI-HZs, tidal locking is relatively unlikely (although it may still occur at a later evolutionary time), whereas for planets around cooler stars, tidal locking is expected to have happened – even though it should be pointed out that tidal locking by itself does not necessarily exclude habitability (e.g., Barnes et al. 2008), although its absence leads to more thermally balanced planetary climates. However, tidal-locking reduces the rotation period of the planet and thus possibly reduces the planet’s protective geomagnetic field. Without a robust magnetic field, ion-pick up mechanisms, combined with strong X-ray–UV radiation, strong winds, and flares, could strip the planet of its atmosphere (e.g., Lammer et al. 2008). On the other hand, Driscoll & Barnes (2015) showed that tidally-locked terrestrial planets could have their geomagnetic fields sustained (or even enhanced) from the tidal heating of their iron-nickel cores.

Another reason why K-dwarfs are expected to provide habitable environments stems from recent planetary geodynamic studies. Haqq-Misra et al. (2016) investigated the impact of limit cycles on the width of stellar habitable zones. Limit cycles mean that planets positioned in the CLI-HZs cannot maintain stable, warm climates, but rather should oscillate between long, globally glaciated states and shorter periods of climatic warmth. Haqq-Misra et al. (2016) argue that such conditions, similar to those experienced on Earth (“Snowball Earth”) would be disadvantageous to the development of complex life, including intelligent life. Thus, limit cycles reduce the usable extent of CLI-HZs as they compromise habitability for planets near the CLI-HZs’ outer rim. The authors point out that for planets around K and M dwarfs, limit cycles should not occur, thus allowing to foster habitable environments based on this criterion. However, Haqq-Misra et al. (2016) view M-dwarfs as less suitable for exolife in part based on the same reasoning as conveyed in this study.

Clearly, the search for planets around different types of stars continues at an unprecedented pace. A fairly recent example includes the detection of a possible Earth-mass planet by Dumusque et al. (2012) orbiting α Cen B (K1 V), a member of the closest stellar system to the Sun, albeit this planet orbits very close to the star is not located within the CLI-HZ. Furthermore, five possible super-Earth planets have been reported to orbit the nearby G8.5 V star τ Ceti (Tuomi et al. 2013). Two of these large Earth-size planet candidates (i.e., τ Ceti e and f) orbit near the inner and outer boundaries of this old star’s continuously habitable zone (Pagano et al. 2015) and are thus potentially habitable. Terrestrial-size planets have also been reported for several other nearby orange dwarfs as well as from the *Kepler* Mission⁵. Finding habitable planets around low-mass K–M stars continues to be a challenging task due to the impacts of the stellar radiative environments, intense plasma fluxes, and the narrowness of the CLI-HZs. Additional planets are expected from the extended *Kepler* Mission (K2), continuing and new high precision spectroscopic radial velocity studies, as well as from the *Transiting Exoplanet Survey Satellite* (TESS) and Gaia.

However, it is noteworthy that recent statistical analyses of *Kepler* Mission exoplanet data indicate that a significant fraction (i.e., 15% – 25%) of red dwarfs is expected to host terrestrial-size planets within their CLI-HZs (e.g., Bonfils et al. 2013; Dressing & Charbonneau 2013, 2015). This implies that tens of billions Earth-size planets in the Milky Way alone hosted by M-dwarfs could have a chance of being potentially habitable, even though potential life forms would most likely constitute extremophiles by terrestrial standards. Possible scenarios include that these potentially habitable planets could have escaped the strong X-ray–UV radiation of their host stars by forming beyond the stellar CLI-HZs. Thereafter, they could have migrated into the CLI-HZs when their host stars had become older and less active. Another possibility is that the planets could have lost their original atmospheres and water inventories at a much later time (ages > 2 Gyr), outgassed and/or captured water and gases from collisions with icy bodies (i.e., exocomets) (e.g., Bosiek et al. 2016). It is also possible that some planets could have been protected by strong geomagnetic fields, shielding them from the expected strong X-ray–UV radiation and winds from their host stars when those were young and highly active (e.g., Khodachenko et al. 2007; Erkaev et al. 2013).

In conclusion, our study indicates that the very high levels of X-ray and FUV radiation experienced by close-in CLI-HZ planets of cool stars, especially red dwarfs, is expected to have negative (detrimental) consequences on the development of life on such planets. All GHZ planets hosted by G–K–M stars experience high levels of X-ray–UV irradiances when the host stars are young (< 0.5 Gyr), including early Earth. However, as discussed in this pa-

⁵For further information, see Planetary Habitability Laboratory, <http://phl.upr.edu>.

per, the close-in GHZ planets hosted by late-K and M dwarfs experience at least an order of magnitude higher levels ionizing radiation and far more extended periods than the Earth. To make matters worse, there is a greater likelihood of large flares from young stars. The levels of the resulting ionizing X-ray–UV radiation and energetic plasmas from flares could erode or eliminate the planet’s atmosphere and water inventories, thus greatly reducing the suitability of the planet for sustained life. These effects as well as other factors (including biological and chemical bottlenecks, asteroid bombardments, among others), as recently discussed by Chopra & Lineweaver (2016) and references therein, could greatly diminish the likelihood of development of multicellular complex life. The lack of evidence of technologically advanced civilizations such as radio signals and other modes of one-way communication are referred to as the Fermi’s Paradox, which continues to remain unresolved (see Chopra & Lineweaver 2016). As discussed in this paper, decisive impediments (roadblocks) to life could be attributable to high energy radiation, strong stellar winds and flares experienced by planets during the first billion years after formation.

This research is supported by the NSF and NASA through grants NSF/RUI-1009903, HST-GO-13020.001-A and Chandra Award GO2-13020X to Villanova University (E. F. G.). We are very grateful for this support. Furthermore, it has been supported in part by NASA through the American Astronomical Society’s Small Research Grant Program as well as the SETI Institute (M. C.). We also wish to acknowledge the availability of HST data through the MAST website hosted by the Space Telescope Science Institute and the Chandra X-ray data through the HEASARC website hosted by the Astrophysics Science Division at NASA/GSFC and the High Energy Astrophysics Division of the Smithsonian Astrophysics Observatory (SAO). Furthermore, we would like to thank an anonymous referee for her/his useful suggestions allowing us to improve the manuscript. This research made use of public databases hosted by SIMBAD, and maintained by CDS, Strasbourg, France. Moreover, we wish to acknowledge assistance by Zhaopeng Wang with computer graphics.

Facilities: ROSAT, XMM-Newton, Chandra, HST (COS), *Kepler*

REFERENCES

- Airapetian, V. S., & Usmanov, A. V. 2016, *ApJ*, 817, L24
- Airapetian, V. S., Glocer, A., Gronoff, G., Hébrard, E., & Danchi, W. 2016, *Nature Geoscience*, 9, 452
- Barnes, R., Raymond, S. N., Jackson, B., & Greenberg, R. 2008, *Astrobiol.*, 8, 557
- Basri, G., Marcy, G. W., & Graham, J. R. 1996, *ApJ*, 458, 600
- Bonfils, X., Delfosse, X., Udry, S., et al. 2013, *A&A*, 549, 109
- Bosiek, K., Hausmann, M., & Hildenbrand, G. 2016, *Astrobiol.*, 16, 311
- Candelaresi, S., Hillier, A., Maehara, H., Brandenburg, A., & Shibata, K. 2014, *ApJ*, 792, 67
- Chabrier, G. 2003, *PASP*, 115, 763
- Chabrier, G., Baraffe, I., Allard, F., Hauschildt, P. H. 2005, Invited Review “Resolved Stellar Populations”, Cancun, April 2005; eprint arXiv:astro-ph/0509798
- Charbonneau, P., Schrijver, C. J., & MacGregor, K. B. 1997, in *Cosmic winds and the heliosphere*, ed. J. R. Jokipii, C. P. Sonett, & M. S. Giampapa (Tucson, AZ: University of Arizona), 677
- Chopra, A., & Lineweaver, C. H. 2016, *Astrobiol.*, 16, 7
- Clark, P. C., Bonnell, I. A., & Klessen, R. S. 2008, *MNRAS*, 386, 3
- Cockell, C. S. 1999, *Icarus*, 141, 399
- Cranmer, S. R., & Saar, S. H. 2011, *ApJ*, 741, A54
- Cuntz, M. 2014, *ApJ*, 780, A14
- Cuntz, M. 2015, *ApJ*, 798, A101
- Davenport, J. R. A., Becker, A. C., & Kowalski, A. F. 2012, *ApJ*, 748, 58
- do Nascimento, J.-D., Jr., Vidotto, A. A., Petit, P., et al. 2016, *ApJ*, 820, L15
- Dressing, C. D., & Charbonneau, D. 2013, *ApJ*, 767, 95
- Dressing, C. D., & Charbonneau, D. 2015, *ApJ*, 807, 45

- Driscoll, P. E., & Barnes, R. 2015, *Astrobiol.*, 15, 739
- Dumusque, X., Pepe, F., Lovis, C., et al. 2012, *Nature*, 491, 207
- Erkaev, N. V., Lammer, H., Odert, P., et al. 2013, *Astrobiol.* 13, 1011
- Fairén, A. G., Davila, A. F., Lim, D., et al. 2010, *Astrobiol.* 10, 821
- Feigelson, E., Townsley, L., Güdel, M., & Stassun, K. 2007, in *Protostars and Planets V*, ed. B. Reipurth, D. Jewitt, & K. Keil (Tucson, AZ: University of Arizona), 313
- France, K., Froning, C. S., Linsky, J. L., et al. 2013, *ApJ*, 763, A149
- Grießmeier, J.-M., Stadelmann, A., Penz, T., et al. 2004, *A&A*, 425, 753
- Güdel, M. 2007, *Liv. Rev. Sol. Phys.*, 4, 3
- Güdel, M., Guinan, E. F., & Skinner, S. L. 1997, *ApJ*, 483, 947
- Guinan, E. F., & Ribas, I. 2002, in *The Evolving Sun and Its Influence on Planetary Environments*, ed. B. Montesinos, A. Gimenez, & E. F. Guinan (San Francisco, CA: ASP), 269, 85
- Guinan, E. F., Ribas, I., & Harper, G. M. 2003, *ApJ*, 594, 561
- Guinan, E. F., Engle, S. G., & Durbin, A. 2016, *ApJ*, 821, A81
- Haqq-Misra, J., Kopparapu, R. K., Batalha, N. E., Harman, C. E., & Kasting, J. F. 2016, *ApJ*, in press; arXiv:1605.07130
- Hawley, S. L., Allred, J. C., Johns-Krull, C. M., et al. 2003, *ApJ*, 597, 535
- Henry, T. 2009, 76th Ann. Meeting Southeastern Sect. of the APS, Abstract #HB.002
- Henry, T. J., & Jao, W.-C. 2015, IAU General Assembly, Meeting #29, Abstract #2253773
- Hillenbrand, L. A., & Carpenter, J. M. 2000, *ApJ*, 540, 236
- Holland, H. D. 1984, *The Chemical Evolution of the Atmosphere and Oceans*, Princeton Series in Geochemistry
- Horner, J., & Jones, B. W. 2010, *IJAsB*, 9, 273
- Husser, T.-O., Wende-von Berg, S., Dreizler, S., Homeier, D., Reiners, A., Barman, T., & Hauschildt, P. H. 2013, *A&A*, 553, A6

- Johnstone, C. P., Güdel, M., Stökl, A., et al. 2015, *ApJ*, 815, L12
- Kaltenegger, L., Miguel, Y., & Rugheimer, S. 2012, *IJAsB*, 11, 297
- Kasting, J. F., Whitmire, D. P., & Reynolds, R. T. 1993, *Icarus*, 101, 108
- Kasting, J. F., Kopparapu, R., Ramirez, R. M., & Harman, C. E. 2014, *Proc. Nat. Aca. Sci.*, 111, 12641
- Katsova, M. M., & Livshits, M. A. 2015, *Sol. Phys.*, 290, 3663
- Keppens, R., MacGregor, K. B., & Charbonneau, P. 1995, *A&A*, 294, 469
- Khodachenko, M. L., Ribas, I., Lammer, H., et al. 2007, *Astrobiol.*, 7, 167
- Kopparapu, R. K., Ramirez, R., Kasting, J. F., et al. 2013, *ApJ*, 765, A131; Erratum 770, A82
- Kopparapu, R. K., Ramirez, R. M., SchottelKotte, J., et al. 2014, *ApJ*, 787, L29
- Kroupa, P. 2001, *MNRAS*, 322, 231
- Kroupa, P. 2002, *Science*, 295, 82
- Kulikov, Yu. N., Lammer, H., Lichtenegger, H. I. M., et al. 2006, *P&SS*, 54, 1425
- Lammer, H. 2007, *Astrobiol.*, 7, 27
- Lammer, H., Selsis, F., Ribas, I., et al. 2003, *ApJ*, 598, L121
- Lammer, H., Kasting, J. F., Chassefière, E., Johnson, R. E., Kulikov, Yu. N., & Tian, F. 2008, *Space Sci. Rev.*, 139, 399
- Lammer, H., Bredehöft, J. H., Coustenis, A., et al. 2009, *A&A Rev.* 17, 181
- Lammer, H., Blanc, M., Benz, W., et al. 2013, *Astrobiol.* 13, 793
- Linsky, J. L., France, K., & Ayres, T. 2013, *ApJ*, 766, 69
- Lissauer, J. J. 2007, *ApJ*, 660, L159
- Lucas, P. W., & Roche, P. F. 2000, *MNRAS*, 314, 858
- Luger, R., & Barnes, R. 2015, *Astrobiol.*, 15, 119
- Luhman, K. L., Rieke, G. H., Young, E. T., et al. 2000, *ApJ*, 540, 1016

- Maehara, H., Shibayama, T., Notsu, S., et al. 2012, *Nature*, 485, 478
- Maehara, H., Shibayama, T., Notsu, Y., et al. 2015, *Earth, Planets and Space*, 67, A59
- Mamajek, E. E., & Hillenbrand, L. A. 2008, *ApJ*, 687, 1264
- Mann, A. W., Gaidos, E., & Ansdell, M. 2013, *ApJ*, 779, A188
- Mayor, M., & Queloz, D. 1995, *Nature*, 378, 355
- Meynet, G., Mermilliod, J.-C., & Maeder, A. 1993, *ApJS*, 98, 477
- Micela, G., Sciortino, S., Vaiana, G. S., Harnden, F. R., Jr., Rosner, R., & Schmitt, J. H. M. M. 1990, *ApJ*, 348, 557
- Miguel, Y., Kaltenegger, L., Linsky, J. L., & Rugheimer, S. 2015, *MNRAS*, 446, 345
- Miller, G. E., & Scalo, J. M. 1979, *ApJS*, 41, 513
- Mowlavi, N., Eggenberger, P., Meynet, G., et al. 2012, *A&A*, 541, A41
- Muench, A. A., Lada, E. A., Lada, C. J. 2000, *ApJ*, 533, 358
- Pagano, M., Truitt, A., Young, P. A., & Shim, S.-H. 2015, *ApJ*, 803, A90
- Penz, T., & Micela, G. 2008, *A&A*, 479, 579
- Perryman, M. A. C., Brown, A. G. A., Lebreton, Y., et al. 1998, *A&A*, 331, 81
- Preusse, S., Kopp, A., Büchner, J., & Motschmann, U. 2005, *A&A*, 434, 1191
- Ramirez, R. M., & Kaltenegger, L. 2014, *ApJ*, 797, L25
- Raymond, S. N., Scalo, J., & Meadows, V. S. 2007, *ApJ*, 669, 606
- Ribas, I., Guinan, E. F., Güdel, M., & Audard, M. 2005, *ApJ*, 622, 680
- Robinson, R. D., Wheatley, J. M., Welsh, B. Y., et al. 2005, *ApJ*, 633, 447
- Rothschild, L. J., & Mancinelli, R. L. 2001, *Nature*, 409, 1092
- Rugheimer, S., Kaltenegger, L., Zsom, A., Segura, A., & Sasselov, D. 2013, *Astrobiol.*, 13, 251
- Rushby, A. J., Claire, M. W., Osborn, H., & Watson, A. J. 2013, *Astrobiol.*, 13, 833
- Salpeter, E. E. 1955, *ApJ*, 121, 161

- Sato, S., Cuntz, M., Guerra Olvera, C. M., Jack, D., & Schröder, K.-P. 2014, *IJAsB*, 13, 244
- Scalo, J., Kaltenegger, L., Segura, A. G., et al. 2007, *Astrobiol.*, 7, 85
- Schrijver, C. J., DeRosa, M. L., & Title, A. M. 2003, *ApJ*, 590, 493
- Schröder, K.-P., & Smith, R. C. 2008, *MNRAS*, 386, 155
- Segura, A., Kasting, J. F., Meadows, V., et al. 2005, *Astrobiol.*, 5, 706
- Segura, A., Walkowicz, L. M., Meadows, V., Kasting, J., & Hawley, S. 2010, *Astrobiol.*, 10, 751
- Selsis, F., Kasting, J. F., Levrard, B., Paillet, J., Ribas, I., & Delfosse, X. 2007, *A&A*, 476, 1373
- Shibayama, T., Maehara, H., Notsu, S., et al. 2013, *ApJS*, 209, 5
- Stern, R. A., Schmitt, J. H. M. M., & Kahabka, P. T. 1995, *ApJ*, 448, 683
- Tarter, J. C., Backus, P. R., Mancinelli, R. L., et al. 2007, *Astrobiol.*, 7, 30
- Tian, F. 2013, in *Lunar and Planetary Science Conference*, Vol. 44, LPI Contribution No. 1719, 1953
- Tian, F., & Ida, S. 2015, *Nature Geoscience*, 8, 177
- Tu, L., Johnstone, C. P., Güdel, M., & Lammer, H. 2015, *A&A*, 577, L3
- Tuomi, M., Anglada-Escudé, G., Gerlach, E., et al. 2013, *A&A*, 549, A48
- Underwood, D. R., Jones, B. W., & Sleep, P. N. 2003, *IJAsB*, 2, 289
- Vidal-Madjar, A., Lecavelier des Etangs, A., Désert, J.-M., et al. 2003, *Nature*, 422, 143

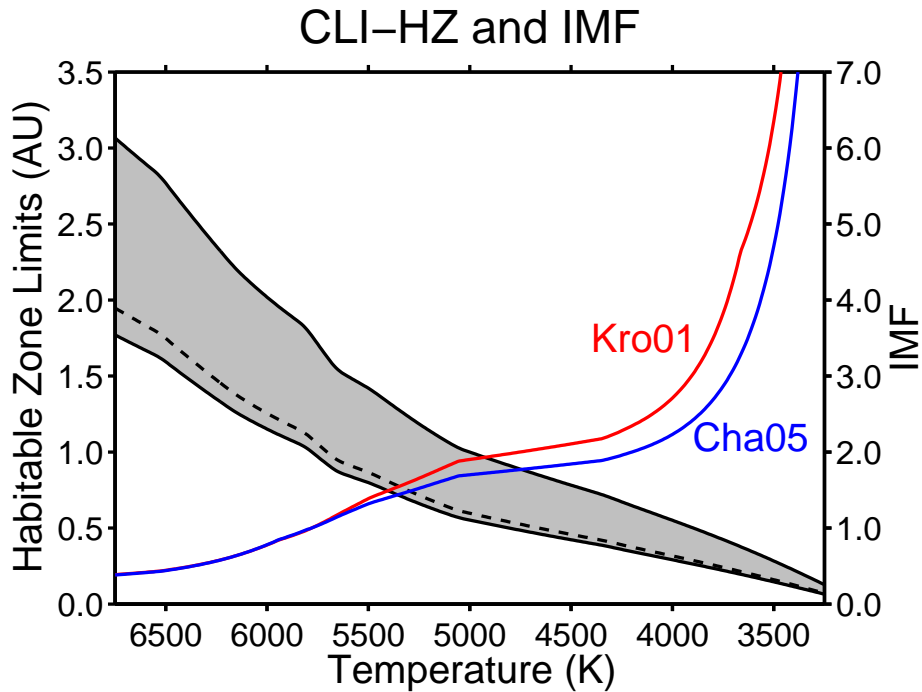


Fig. 1.— Inner and outer limits of the CLI-HZ, represented by the GHZ (black lines) with its extent depicted as grayish area. The HTDs are depicted as well (dashed line). Additionally, we show the behavior of the IMF (normalized to unity for $1 M_{\odot}$) as given by Kroupa (2001) (red line) and Chabrier et al. (2005) (blue line). Also note that IMF does not flatten near $0.5 M_{\odot}$ if displayed against the stellar effective temperature, though it does if displayed against $\log M$ (with M as stellar mass), the most customary approach.

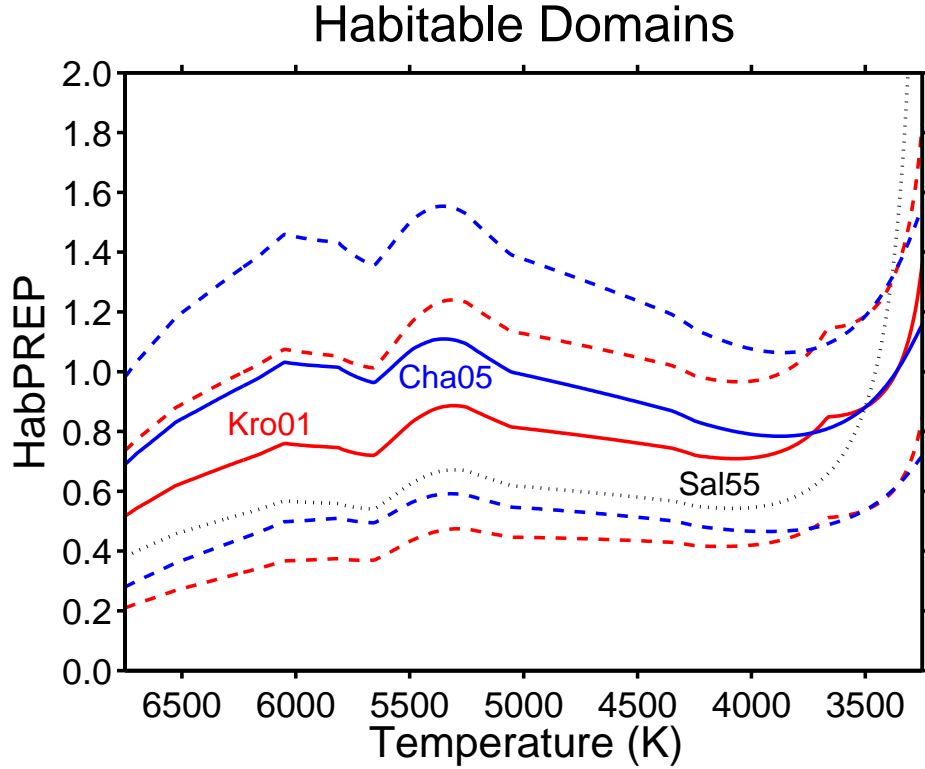


Fig. 2.— HabPREP values depicted as function of the stellar effective temperature with the IMF chosen after Kroupa (2001) (red) and Chabrier et al. (2005) (blue). Results are given regarding the GHZ (solid lines), RVEM (dashed lines, top), and the CHZ (dashed lines, bottom). For comparison and historic reasons, the HabPREP values for the GHZ have also been given regarding the IMF of Salpeter (1955) (dotted line). Note that the overall behavior of HabPREP shows little dependence on the type of the CLI-HZ, i.e., RVEM, GHZ, or CHZ.

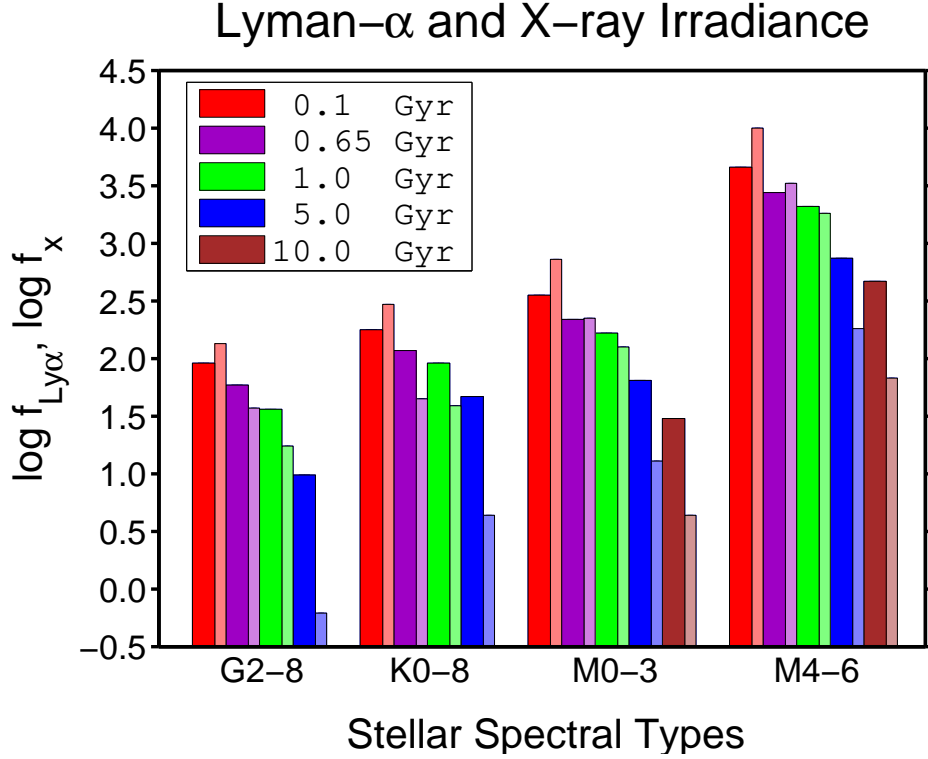


Fig. 3.— Lyman- α and X-ray irradiances (in $\text{ergs s}^{-1}\text{cm}^{-2}$) for different sets of main-sequence stars regarding planets located at HTDs. Stellar ages of about 0.1, 0.65, 1.0, 5.0, and 10 Gyr are represented by the colors *red*, *purple*, *green*, *blue*, and *brown*, respectively. Large-width bars indicate the results for Lyman- α , whereas small-width bars (with slightly lesser bright colors) convey the results for the X-ray irradiances. Note that the y -axis uses logarithmic units, allowing us to display the drastic increase of both $f_{\text{Ly}\alpha}$ and f_x between G dwarfs and late M dwarfs. For the various G, K and M spectral type bins, the X-ray and FUV Ly- α HTD fluxes all increase with decreasing stellar age. The increase of the HTD X-ray flux from 0.1 to 5.0 Gyr is up to 500 times, whereas for the same age range, the increase in FUV Ly- α HTD fluxes is much less (see also Table 3). The latter is typically ~ 5 –10 times larger for young stars than for old stars. Moreover, the X-ray and FUV Ly- α HTD fluxes for stars of similar ages from G2-8 dwarfs to M4-6 dwarfs increase over 100–500 times. Thus HTD planets hosted by an M4-6 dwarfs (due to the very small HTDs) have extremely high levels of X-ray and FUV irradiances, particularly when young.

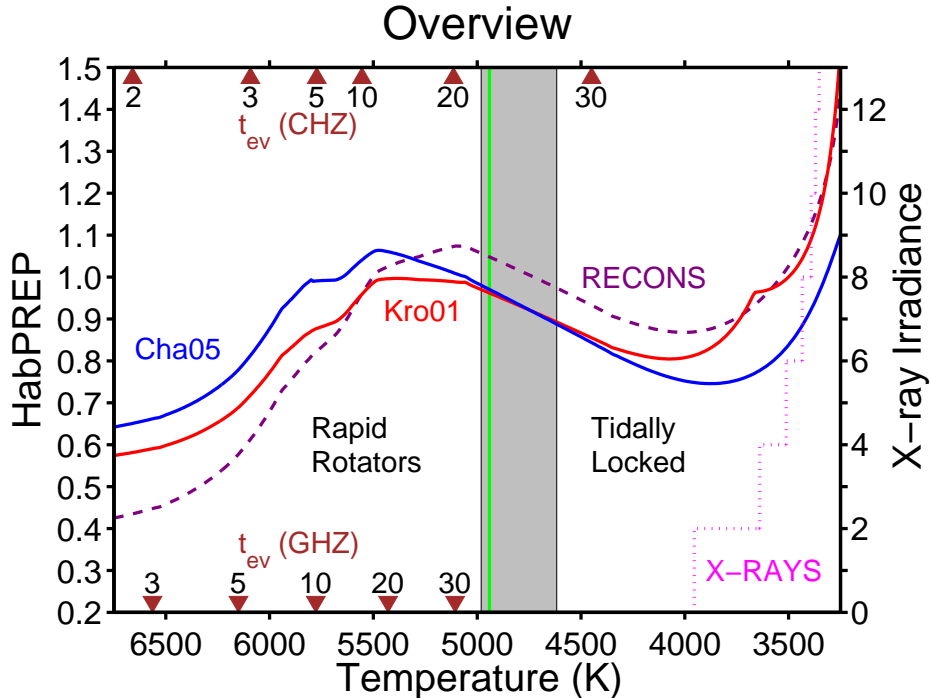


Fig. 4.— Depiction of various functions and quantities, indicating the significance (suitability) of late-G (\sim G8 V) to mid-K (\sim K5 V) type stars (i.e., “dwarf orange stars”) for exobiology. The normalized habitable real estate, defined on the left y -axis of the plot by the product of the initial mass function and the HZ extent ($\text{IMF} \times \text{HZ}$) is displayed versus the stellar effective temperature. As shown, the amount of habitable planetary real estate, HabPREP, with the IMF given by Kroupa (2001) and Chabrier et al. (2005) as well as based on the results from the RECONS project (see text), forms an aggregate maximum at the temperature range for orange dwarfs. We also convey the values of t_{ev} (in Gyr) for the CHZ and GHZ, describing the timescales of stability for the continuous habitable zone (with data beyond 30 Gyr disregarded). For a tidal locking timescale of 4.5 Gyr, we show the domain for the onset of tidal locking for planets located in the GHZs (grayish area). The dividing line (green) separates tidal locking and fast rotations for planets at HTDs. Moreover, in the form of a histogram (magenta) defined on the right y -axis of the plot, we show domains of possible exobiological exclusion owing to high levels of X-ray irradiance. We report distinct factors of enhancements in $f_X(650 \text{ Myr})$ for planets at HTDs relative to a solar-type G2 V star of that age. For example, the values for X-ray irradiance are found to be about $2\times$, $5\times$, and $10\times$ higher for stars of $T_{\text{eff}} \simeq 3950 \text{ K}$ (\sim K8 V), 3570 K (\sim M2 V), and 3390 K (\sim M3 V), respectively. Factors larger than 100 are identified for stars of $T_{\text{eff}} < 3085 \text{ K}$ (\sim M5 V). For the latter, the CLI-HZ is very close ($< 0.05 \text{ au}$) to the host star.

Table 1. Habitable Zone Limits and Definitions

Description	Models		Definitions		
	Kas93	Kop1314	Kas93	Kop1314	This work
...					
Recent Venus	0.75	0.75	RVEM	optimistic	RVEM
Runaway greenhouse effect	0.84	0.95	GHZ	conservative	GHZ
Moist greenhouse effect	0.95	0.99	CHZ	...	CHZ*
First CO ₂ condensation	1.37	...	CHZ	...	CHZ*
Maximum greenhouse effect	1.67	1.68	GHZ	conservative	GHZ
Early Mars	1.77	1.77	RVEM	optimistic	RVEM

Note. — Considering that the “first CO₂ condensation” limit is not supported by the work of Kopparapu et al. (2013, 2014) reduces the relevance of the CHZ, hence labelled as (*). Nevertheless, we still convey this limit to allow comparisons with previous work. Kopparapu et al. (2013) use the terms “optimistic” and “conservative” limits; however, in several previous studies those limits were identified as the GHZ and CHZ limits, respectively, rather than the RVEM and GHZ limits.

Table 2. CLI-HZ Evolutionary Time Scales and Limits

Sp. Type	T_{eff}	t_{ev}		CLI-HZ Limits		
		CHZ (Gyr)	GHZ (Gyr)	CHZ (au)	GHZ (au)	RVEM (au)
...	...	CHZ	GHZ	CHZ	GHZ	RVEM
...	(K)	(Gyr)	(Gyr)	(au)	(au)	(au)
F0	7100	1.4	2.1	2.32 – 2.87	2.16 – 3.72	1.70 – 3.93
F2	6830	1.8	2.4	1.97 – 2.51	1.85 – 3.20	1.46 – 3.37
F5	6530	2.3	3.1	1.72 – 2.24	1.62 – 2.82	1.28 – 2.97
F8	6150	2.8	5.0	1.33 – 1.78	1.26 – 2.21	1.00 – 2.33
G0	5940	3.7	7.5	1.17 – 1.58	1.11 – 1.96	0.88 – 2.06
G2	5780	4.8	9.9	0.99 – 1.36	0.95 – 1.68	0.75 – 1.77
G5	5670	7.8	13.9	0.91 – 1.26	0.87 – 1.55	0.69 – 1.63
G8	5460	11.8	19.2	0.82 – 1.14	0.79 – 1.40	0.62 – 1.48
K0	5250	16.0	24.8	0.69 – 0.98	0.67 – 1.20	0.53 – 1.27
K2	5050	21.9	32.0	0.59 – 0.84	0.57 – 1.02	0.45 – 1.08
K5	4410	30.4	41.4	0.39 – 0.58	0.38 – 0.70	0.30 – 0.74
K8	4000	>50	>50	0.27 – 0.41	0.26 – 0.49	0.21 – 0.52
M0	3800	>100	>100	0.22 – 0.34	0.21 – 0.41	0.17 – 0.43

Table 3. Planetary Lyman- α and X-ray Irradiance for G, K and M Dwarfs

T_{eff} (K)	HTD (au)	0.1 Gyr (ergs s ⁻¹ cm ⁻²)		0.65 Gyr (ergs s ⁻¹ cm ⁻²)		1.0 Gyr (ergs s ⁻¹ cm ⁻²)		5.0 Gyr (ergs s ⁻¹ cm ⁻²)		10 Gyr (ergs s ⁻¹ cm ⁻²)	
...	...	$f_{\text{Ly}\alpha}$	f_{X}	$f_{\text{Ly}\alpha}$	f_{X}	$f_{\text{Ly}\alpha}$	f_{X}	$f_{\text{Ly}\alpha}$	f_{X}	$f_{\text{Ly}\alpha}$	f_{X}
5780	$\equiv 1$	75.5	112	49.2	32.5	29.2	14.2	6.60	0.224
5500	0.866	101	149	65.6	43.3	38.9	18.9	8.80	0.299
5300	0.745	97	146	63.8	35.5	41.4	18.5	13.9	1.32
5000	0.597	101	155	67.2	27.4	48.9	19.7	23.6	1.80
4800	0.539	111	171	74.0	23.6	57.4	21.9	30.2	2.51
4600	0.433	172	265	115	36.6	89.0	34.0	46.8	3.89
4200	0.375	191	354	127	48.8	98.3	45.3	50.7	5.19
3900	0.287	235	389	154	70.5	120	54.3	59.7	6.00
3600	0.194	293	560	186	147	142	90.2	61.9	9.47	17.8	2.58
3400	0.126	410	901	249	300	188	162	66.4	16.4	42.2	6.11
3200	0.053	2318	5091	1404	1694	1063	917	375	92.6	239	34.5
3000	0.031	6777	14886	4107	4955	3107	2682	1097	271	697	101

Note. — The fluxes pertain to distances given by the HTDs.